

# Postprandial increase of oleoylethanolamide mobilization in small intestine of the Burmese python (*Python molurus*)

Giuseppe Astarita<sup>1,2</sup>, Bryan C. Rourke<sup>3</sup>, Johnnie B. Andersen<sup>4</sup>, Jin Fu<sup>1,2</sup>, Janet H. Kim<sup>1</sup>,  
Albert F. Bennett<sup>5</sup>, James W. Hicks<sup>5</sup>, Daniele Piomelli<sup>1,2,6</sup>

<sup>1</sup>Department of Psychiatry and Human Behavior, University of California, Irvine, CA,  
USA 92697

<sup>2</sup>Center for Drug Discovery, University of California, Irvine, CA, USA 92697

<sup>3</sup>Department of Biological Sciences, California State University, Long Beach, CA, USA  
90840

<sup>4</sup>Department of Zoophysiology, University of Aarhus, DK-8000 Aarhus, Denmark

<sup>5</sup>Department of Ecology and Evolutionary Biology, University of California, Irvine, CA,  
USA 92697

<sup>6</sup>Department of Pharmacology, University of California, Irvine, CA, USA 92697

## Contact information:

Daniele Piomelli, Department of Pharmacology, 3101 Gillespie NRF, University of  
California, Irvine, CA 92697-4625. E-mail: piomelli@uci.edu

**ABSTRACT**

Oleylethanolamide (OEA) is an endogenous lipid mediator that inhibits feeding in rats and mice by activating the nuclear receptor peroxisome proliferator-activated receptor- $\alpha$  (PPAR- $\alpha$ ). In rodents, intestinal OEA levels increase about 3-fold upon refeeding, a response that may contribute to the induction of between-meal satiety. Here we examined whether feeding-induced OEA mobilization also occurs in Burmese pythons (*Python molurus*), a species of ambush-hunting snakes that consumes huge meals after months of fasting and undergoes massive feeding-dependent changes in gastrointestinal hormonal release and gut morphology. Using liquid-chromatography/mass-spectrometry (LC/MS), we measured OEA levels in the gastrointestinal tract of fasted (28 days) and fed (48h after feeding) pythons. We observed a nearly 300-fold increase in OEA levels in the small intestine of fed compared to fasted animals ( $322 \pm 121$  vs  $1 \pm 1$  pmol/mg protein,  $n=3-4$ ). *In situ* OEA biosynthesis was suggested by the concomitant increase of N-acyl phosphatidylethanolamine species that serve as potential biosynthetic precursors for OEA. Furthermore, we observed a concomitant increase in saturated, mono- and di-unsaturated, but not polyunsaturated fatty-acid ethanolamides (FAE) in the small intestine of fed pythons. The identification of OEA and other FAEs in the gastrointestinal tract of *Python molurus* suggests that this class of lipid messengers may be widespread among vertebrate groups and may represent an evolutionarily ancient means of regulating energy intake.

Keywords: OEA, peroxisome proliferator-activated receptor- $\alpha$  (PPAR- $\alpha$ ), anandamide, fatty-acid ethanolamide (FAE), digestive system, food intake.

## INTRODUCTION

The gastrointestinal tract plays a pivotal role in the regulation of vertebrate feeding and digestion, controlling multiple aspects of this process through both neuronal and humoral mechanisms. Among the humoral signals released by the gut, peptides such as cholecystokinin, glucagon-like peptide-1 and ghrelin have attracted the most attention (4), but recent evidence suggests that lipid messengers also are involved (7, 18). One such messenger, oleoylethanolamide (OEA) – the amide of oleic acid and ethanolamine – is synthesized in a variety of rodent tissues, including the small intestine, where its levels decrease during food deprivation and increase upon refeeding (24). These periprandial fluctuations, which likely result from local changes in OEA biosynthesis and hydrolysis, are thought to represent a previously undescribed satiety-modulating signal. In support of this idea, pharmacological studies have shown that systemic administration of OEA produces profound anorexiant effects in rats and mice (11, 17, 19, 21, 24). These actions appear to be behaviorally selective, as they cannot be attributed to induction of malaise, anxiety, stress or motor inhibition (21, 24). Furthermore, meal-pattern analyses in free-feeding rats suggest that, when administered as a drug, OEA modulates food intake by selectively prolonging the interval between successive meals, rather than by accelerating the termination of individual meals (11, 19). Thus, the anorexiant effects of this lipid mediator are strikingly different from those of the gut peptide cholecystokinin (CCK), which reduces feeding by shortening meal size and duration (23).

The nuclear receptor peroxisome proliferator-activated receptor- $\alpha$  (PPAR- $\alpha$ ) is a key regulator of lipid metabolism and energy balance in mammals (8, 15). Three lines of evidence indicate that this receptor, which is abundantly expressed in the intestine (2, 3), mediates the effects of OEA. Firstly, OEA binds with high affinity to the purified ligand-binding domain satiety-inducing of mouse and human PPAR- $\alpha$  ( $K_D$  37 and 40 nM,

respectively) and activates with high potency PPAR- $\alpha$ -driven transactivation in heterologous expression systems (half-maximal effective concentration, EC<sub>50</sub> 120 nM) (10). Secondly, synthetic PPAR- $\alpha$  agonists, such as the compounds GW7647 and Wy-14643, exert anorexiant effects that are behaviorally identical to those produced by OEA (10). Thirdly, mutant mice in which the PPAR- $\alpha$  gene has been deleted by homologous recombination (PPAR- $\alpha$ <sup>-/-</sup> mice) do not respond to OEA or synthetic PPAR- $\alpha$  agonists, although they retain normal anorexiant responses to CCK octapeptide and fenfluramine (10). Together, these findings suggest that OEA is a lipid mediator produced in the small intestine, which regulates feeding behavior by activating local PPAR- $\alpha$ . The precise sequence of events that leads from intestinal PPAR- $\alpha$  activation to induction of satiety remains unclear. However, the finding that either subdiaphragmatic vagotomy or treatment with the neurotoxin capsaicin abrogates OEA-induced hypophagia suggests that this process is mediated by afferent sensory signals (9).

At present, all information on the OEA response is derived from experiments in rodents. It is unknown how primitive or phylogenetically widespread this regulatory system is. Further, it is unknown how responsive this system is to meal size or frequency. To begin to address these issues, we examined the OEA response to feeding and digestion in an ectothermic vertebrate, the Burmese python (*Python molurus*). This snake species provides an excellent model organism in which to study digestive physiology on account of the great rapidity and magnitude of its physiological responses to feeding (1, 26). Most mammals, including rats and humans, consume small meals at frequent intervals and display relatively modest regulatory responses to food intake. By contrast, Burmese pythons and other ambush-hunting snakes can consume huge meals (up to 50-60% of their own body mass) after months of fasting and must mount, therefore, adequate regulatory responses to cope with these events (25). For example, postprandial

increases in plasma CCK levels are much larger in pythons (25 fold) than they are in rats (3 fold) (27). Exceedingly large post-feeding responses have also been observed with other gastrointestinal peptides, including glucagon, glucose-dependent insulinotropic peptide and neurotensin (27).

We hypothesized that feeding in Burmese pythons may cause an increase in intestinal OEA mobilization similar to that previously reported for gut peptides. To test this idea, we measured levels of OEA and its phospholipid precursors, N-acyl phosphatidylethanolamine (NAPE) (6), in gastrointestinal segments of fasted and fed pythons.

## MATERIAL AND METHODS

**Animals and tissue collection.** We obtained seven Burmese pythons (*Python molurus*) of undetermined sex with a body mass ranging from 0.503-1.286 kg (average weight,  $0.729 \pm 0.043$  kg) from a commercial supplier (Bob Clark Captive Bred Reptiles, Oklahoma City, OK, USA). The snakes were kept at the University of California, Irvine animal housing facility. They were housed in separate containers at 30°C with free access to water and on a 12h:12h light:dark cycle. The animals were fed rats immediately prior to shipment. Upon arrival, they were fasted for 4 weeks, and then were divided into 2 groups. The first group (n=3) was killed at four weeks without feeding; the second group (n=4) was allowed to eat 1-3 rats equivalent to  $25.0 \pm 0.1$  % of their body mass and sacrificed 48 hours after feeding. Gastrointestinal segments (stomach, proximal small intestine and colon), liver, rib and jaw muscles were removed, rinsed in saline, cut into sections, and flash frozen in liquid nitrogen. All animal experiments were carried out under University of California, Irvine Animal Research Protocol Number 1999-2123 to JWH.

**Chemicals.** We purchased fatty-acid chlorides from Nu-Chek Prep (Elysian, MN); [ $^2\text{H}_4$ ]-ethanolamine from Cambridge Isotope Laboratories (Andover, MA); 1-oleoyl, 2-palmitoyl-*sn*-glycero-phosphoethanolamine-*N*-arachidonoyl from Avanti Polar Lipids (Alabaster, AL). Solvents were from Burdick and Jackson (Muskegon, MI) and all other chemicals from Sigma (St. Louis, MO).

**Chemical syntheses.** We prepared OEA and other fatty-acid ethanolamides (FAEs) by the reaction of fatty-acid chlorides with a 10-fold molar excess of ethanolamine or [ $^2\text{H}_4$ ]-ethanolamine. Reactions were conducted in dichloromethane at 0-4°C for 15 min, with

stirring. The products were washed with water, dehydrated over sodium sulfate, filtered, and dried under N<sub>2</sub>. They were fully characterized by liquid chromatography/mass spectrometry (LC/MS) and <sup>1</sup>H and <sup>13</sup>C nuclear magnetic resonance spectroscopy. The purity was >98%.

**Lipid extractions.** We homogenized tissue samples and measured protein concentration using a Bradford protein assay (Bio-Rad Laboratories Inc., Hercules, CA). We spiked tissue homogenates with standard [<sup>2</sup>H<sub>4</sub>]-OEA, [<sup>2</sup>H<sub>4</sub>]-palmitoylethanolamide (PEA) and [<sup>2</sup>H<sub>4</sub>]-arachidonylethanolamide (anandamide), and subjected them to methanol/chloroform (1:2, v/v) extraction. FAEs and their precursors NAPE were fractionated by open-bed silica gel column chromatography, as previously described (Cadas et al. 1997). Briefly, the lipid extracts were reconstituted in chloroform and loaded onto small columns packed with Silica Gel G (60-Å 230-400 Mesh ASTM; Whatman, Clifton, NJ). FAEs and NAPE were eluted with 9:1 (v/v) and 5:5 (v/v) chloroform/methanol, respectively. Eluates were dried under N<sub>2</sub> and reconstituted in 0.1 ml of chloroform/methanol (1:4, v/v) for further analyses.

**LC/tandem MS (LC/MS/MS) analyses.** We performed LC/MS/MS analyses using an 1100-LC system coupled to a MS detector Ion-Trap XCT (Agilent Technologies, Inc., Palo Alto, CA) interfaced with an electrospray ionization (ESI) chamber. We separated OEA using a XDB Eclipse C<sub>18</sub> column (50x4.6 mm i.d., 1.8 μm, Zorbax). The mobile phase A consisted of water containing 0.25% acetic acid, 5 mM ammonium acetate; the mobile phase B consisted of methanol containing 0.25% acetic acid, 5 mM ammonium acetate. We applied a linear gradient from 85% to 90% of B in 2.5 min at a flow rate of 1.5 ml/min with column temperature at 40°C. MS detection was in the positive ionization mode, capillary voltage was set at 3.5 kV and skimmer voltage at 40V. N<sub>2</sub> was used as

drying gas at a flow rate of 12 liters/min, temperature of 350°C and nebulizer pressure 80 PSI. Capillary exit was set at 115V. For the identification of OEA, we monitored  $m/z$  326  $[M+H]^+$  as precursor ion in  $MS^n$  mode. We applied a fragmentation amplitude of 0.7 V to generate a series of characteristic fragment ions for OEA ( $m/z$  309.3, 265.2, 247.3), using helium as collision gas.

**LC/MS analyses.** We used an 1100-LC system coupled to a 1946A-MS detector (Agilent Technologies, Inc., Palo Alto, CA) equipped with ESI interface. We separated FAEs using a XDB Eclipse  $C_{18}$  column (50x4.6 mm i.d., 1.8  $\mu$ m, Zorbax), eluted with a gradient of methanol in water (from 85% to 90% methanol in 2.5 min) at a flow rate of 1.5 ml/min. Column temperature was kept at 40°C. MS detection was in the positive ionization mode, capillary voltage was set at 3 kV and fragmentor voltage was varied from 120 to 140 V.  $N_2$  was used as drying gas at a flow rate of 13 liters/min and a temperature of 350°C. Nebulizer pressure was set at 60 PSI. We quantified OEA, PEA and anandamide with an isotope-dilution method (12), monitoring sodium adducts of the molecular ions  $[M+Na]^+$  in the selected ion-monitoring (SIM) mode. All other FAEs were quantified using  $[^2H_4]$ -OEA as a standard. We fractionated NAPEs by reversed-phase LC, using a Bondapak  $C_{18}$  column (300x3.9 mm i.d., 10  $\mu$ m, Waters) maintained at 20°C. NAPEs were eluted with a linear gradient of methanol in water (from 75% to 100% in 30 min) with a flow rate of 1.0 ml/min. MS detection was in the negative ionization mode; the capillary voltage was set at 4kV and the fragmentor voltage was at 200V.  $N_2$  was used as drying gas at a flow rate of 12 liters/min and a temperature of 350°C. The nebulizer pressure was set at 30 PSI. We monitored diagnostic ions (deprotonated molecules  $[M-H]^-$ ) in the SIM mode and quantified them using calibration curves constructed with synthetic 1-oleoyl, 2-palmitoyl-*sn*-glycero-phosphoethanolamine-*N*-

arachidonoyl ([M-H]<sup>-</sup>, mass-to-charge ratio (*m/z*) 1003).

**Statistical analyses.** Results are expressed as mean ± S.E.M. The significance of differences among groups was evaluated using Student's *t* test or, when appropriate, two-way analysis of variance (ANOVA) followed by Bonferroni's post-hoc test, with feeding conditions and gastrointestinal segments as the two factors. Analyses were conducted using GraphPad Prism (GraphPad Software, Inc.) and differences were considered significant if *P*<0.05.

## RESULTS

We collected the proximal small intestine from either fasted or fed pythons and identified OEA in lipid extracts by LC coupled to tandem MS. A component eluting from the LC column with a retention time of 2.5 min yielded a precursor ion of  $m/z$  326.3, corresponding to the molecular ion ( $[M+H]^+$ ) for OEA, along with fragment ions of  $m/z$  309.3 ( $[M+H]^+-OH$ ), 265.2 ( $[M+H]^+-NH_2CH_2CH_2OH$ ), 247.3 ( $[M+H]^+-NH_2CH_2CH_2OH-H_2O$ ) (Fig.1A). Retention time and fragmentation pattern of the precursor ion were identical to those obtained with authentic OEA standard (Fig. 1B).

We next quantified OEA levels in different tissues by isotope-dilution LC/MS, monitoring an additional diagnostic ion of  $m/z$  348 ( $[M+Na]^+$ ) (Fig. 2A). OEA levels were about 300-fold higher in the small intestine of fed pythons ( $322\pm 121$  pmol/mg protein,  $n=4$ ) compared with fasted pythons ( $1\pm 1$  pmol/mg protein,  $n=3$ ) (Fig. 2B). Two-way ANOVA gave the following results:  $F(\text{interactions})_{2,15} = 4.990$ ,  $P < 0.05$ ;  $F(\text{feeding conditions})_{1,15} = 7.220$ ,  $P < 0.05$ ;  $F(\text{gastrointestinal sections})_{2,15} = 4.778$ ,  $P < 0.05$ . A Bonferroni's post-hoc test indicated significant differences in OEA levels in the small intestine of fed animals compared with fasted animals ( $P < 0.01$ ). No such difference was noted in the stomach or colon (Fig.2B). Moreover, no significant change in OEA levels was observed in the liver (fasted,  $4.8\pm 1.9$  pmol/mg protein,  $n=3$ ; fed,  $15.6\pm 5.4$  pmol/mg,  $n=4$ ; Student's  $t$  test,  $P=0.13$ ), rib muscle (fasted,  $0.34\pm 0.23$  pmol/mg,  $n=3$ ; fed,  $0.42\pm 0.24$  pmol/mg,  $n=4$ ;  $P=0.33$ ) and jaw muscle (fasted,  $0.40\pm 0.22$  pmol/mg,  $n=3$ ; fed,  $0.70\pm 0.22$  pmol/mg,  $n=4$ ;  $P=0.82$ ).

Next, to determine whether *de novo* OEA biosynthesis contributed to the observed increase in intestinal OEA levels, we quantified two NAPE species, which are thought to serve as OEA precursors (Scheme 1): 1-stearoyl-2-arachidonoyl-*sn*-glycerophosphoethanolamine-*N*-oleoyl (NAPE1,  $m/z$  1029) and 1-oleoyl-2-arachidonoyl-*sn*-

phosphoethanolamine-*N*-oleoyl (NAPE2, *m/z* 1031) (Fig. 3A). Significant postprandial increases in the levels of both NAPE1 and NAPE2 were observed in the small intestine of fed compared with fasted pythons (two-way ANOVA  $F_{1/15} = 26.60$ ,  $P < 0.001$  for NAPE1 and  $F_{1/15} = 10.55$ ,  $P < 0.01$  for NAPE2; Bonferroni's test  $P < 0.001$  for NAPE1 and  $P < 0.05$  for NAPE 2) (Fig. 3B). By contrast, no significant differences in NAPE levels were found in the stomach or colon (Fig. 3B).

Because OEA shares a common biosynthetic pathway with other biologically active FAEs, such as the endogenous cannabinoid anandamide (20) and the PPAR- $\alpha$  agonist PEA (16), we examined whether these lipid mediators are also present in the gastrointestinal tract of the python. The chemical structures of various FAEs identified and quantified in these analyses are reported in Table 1. Identifications were based on the detection of sodium adduct ions  $[M+Na]^+$  of appropriate mass (Table 1) at the retention time of authentic standards (9). As seen with OEA, levels of saturated, mono- and di-unsaturated FAEs, including PEA (16:0), stearoylethanolamide (18:0), palmitoleoylethanolamide (16:1,  $\Delta^9$ ) and linoleoylethanolamide (18:2,  $\Delta^{9-12}$ ), were higher in fed than fasted pythons (two-way ANOVA:  $F_{1/13} = 6.551$ ,  $P < 0.05$  for palmitoylethanolamide;  $F_{1/14} = 14.01$ ,  $P < 0.01$  for stearoylethanolamide;  $F_{1/15} = 8.607$ ,  $P < 0.05$  for linoleoylethanolamide;  $F_{1/15} = 4.706$ ,  $P < 0.05$  for palmitoleoylethanolamide) (Table 1). By contrast, polyunsaturated FAEs, such as anandamide (20:4,  $\Delta^{5-8-11-14}$ ),  $\gamma$ -linolenylethanolamide (18:3,  $\Delta^{6-9-12}$ ), homo- $\gamma$ -linolenylethanolamide (20:3,  $\Delta^{8-11-14}$ ) and docosahexanylethanolamide (22:6,  $\Delta^{4-7-10-13-16-19}$ ) did not significantly change upon feeding (Table 1).

## DISCUSSION

The major result of the present study is that feeding in the Burmese python is accompanied by a profound upregulation of OEA mobilization in the proximal small intestine. Levels of this anorexiant lipid mediator increase over 300 fold following a meal (from  $13\pm 13$  to  $3220\pm 1415$  pmol/g wet tissue). Comparison with rodents, where feeding causes on average a 3-fold elevation in OEA levels (from  $120\pm 15$  to  $350\pm 150$  pmol/g wet tissue) (10, 24), highlights the exceptional magnitude of this response in pythons, and suggests that intestinal OEA mobilization in python is tightly clamped during fasting and massively stimulated upon refeeding.

In mammals, the biosynthesis of OEA and other FAEs requires the activities of two separate enzymes: N-acyltransferase (NAT) and NAPE-specific phospholipase D (NAPE-PLD). NAT catalyzes the transfer of a fatty-acid group from the *sn*-1 position of phosphatidylcholine to the free amine of phosphatidylethanolamine (Scheme 1). This reaction leads to the formation of a family of NAPE species, which are cleaved by NAPE-PLD to produce OEA and other FAEs (Scheme 1). The finding that levels of two putative OEA precursors are significantly increased in the small intestine of fed pythons suggests that feeding stimulates OEA biosynthesis through the NAT/NAPE-PLD pathway. Since we did not measure the enzymatic activities of NAT and NAPE-PLD, we cannot completely rule out the possibility that OEA was derived from a different biochemical route or from exogenous sources such as food. However, two observations make this possibility unlikely. First, significant changes in OEA levels were observed only in the small intestine, although food remains were predominantly found in the stomach. Secondly, while saturated, mono- and di-unsaturated FAEs increased dramatically after feeding, poly-unsaturated FAEs underwent only small, insignificant changes. This finding is consistent with results previously obtained in rodents, in which a

role for the NAPE-PLD pathway in OEA synthesis is well documented (5, 6, 30), and inconsistent with the possibility that OEA originates from the diet.

The differential regulation in the biosynthesis of FAEs with varying degrees of fatty-acid chain unsaturation, though unexplained at the molecular level, may be functionally significant. The mono-saturated and saturated FAEs OEA and PEA are endogenous ligands of the nuclear receptor PPAR- $\alpha$ , which plays a central role in the control of energy balance and lipid metabolism in mammals (8, 15). Thus, the observed increase in the levels of these compounds in the python small intestine may be related to PPAR- $\alpha$  activation. Importantly, PPAR- $\alpha$  expression has been demonstrated in reptiles and other ectothermic vertebrates (14), although the functional roles of this receptor have not yet been investigated. In light of the present results, it would be interesting to explore such roles as well as to determine whether reptilian PPAR- $\alpha$  recognizes the same set of FAEs, which are recognized by mammalian PPAR- $\alpha$ . On the other hand, polyunsaturated FAEs, such as anandamide, selectively bind to G protein-coupled cannabinoid receptors (13, 22). The expression of these receptors in fish, amphibians and birds has been demonstrated (28, 29, 31) and evidence indicates that they are implicated in multiple aspect of behavior (20, 29). The occurrence and physiological roles of cannabinoid receptors in reptiles remains unexplored.

In conclusion, the identification of OEA and other endogenous FAEs in the gastrointestinal tract of the Burmese python reveals that this class of lipid messengers may be widespread across vertebrate groups and possibly of ancient evolutionary origin. The signaling pathways engaged by these mediators might thus represent a common mechanism for the regulation of energy balance in vertebrates.

## ACKNOWLEDGMENTS

We thank Mr. K. Eng for the help with lipid extractions, Dr. J. LoVerme for insightful discussions and Dr. F. Ahmed for consultancy on chromatographic separation. Lipid analyses were conducted at the Agilent/UCI Analytical Discovery Facility, Center for Drug Discovery.

## GRANTS

This work was supported by National Institute of Health grant DK070347 (to D.P.) and by National Science Foundation grant IB-N0091308 (to A.F.B.).

## REFERENCES

1. **Andersen JB, Rourke BC, Caiozzo VJ, Bennett AF, and Hicks JW.** Postprandial cardiac hypertrophy in pythons. *Nature* 434: 37-38, 2005.
2. **Berger J and Moller DE.** The mechanisms of action of PPARs. *Annu Rev Med* 53: 409-435, 2002.
3. **Bocher V, Pineda-Torra I, Fruchart JC, and Staels B.** PPARs: transcription factors controlling lipid and lipoprotein metabolism. *Ann N Y Acad Sci* 967: 7-18, 2002.
4. **Broberger C.** Brain regulation of food intake and appetite: molecules and networks. *J Intern Med* 258: 301-327, 2005.
5. **Cadas H, di Tomaso E, and Piomelli D.** Occurrence and biosynthesis of endogenous cannabinoid precursor, *N*-arachidonoyl phosphatidylethanolamine, in rat brain. *J Neurosci* 17: 1226-1242, 1997.
6. **Cadas H, Gaillet S, Beltramo M, Venance L, and Piomelli D.** Biosynthesis of an endogenous cannabinoid precursor in neurons and its control by calcium and cAMP. *J Neurosci* 16: 3934-3942, 1996.
7. **Cota D, Marsicano G, Tschop M, Grubler Y, Flachskamm C, Schubert M, Auer D, Yassouridis A, Thone-Reineke C, Ortman S, Tomassoni F, Cervino C, Nisoli E, Linthorst AC, Pasquali R, Lutz B, Stalla GK, and Pagotto U.** The endogenous cannabinoid system affects energy balance via central orexigenic drive and peripheral lipogenesis. *J Clin Invest* 112: 423-431, 2003.
8. **Desvergne B and Wahli W.** Peroxisome proliferator-activated receptors: nuclear control of metabolism. *Endocr Rev* 20: 649-688, 1999.

9. **Fegley D, Gaetani S, Duranti A, Tontini A, Mor M, Tarzia G, and Piomelli D.** Characterization of the fatty acid amide hydrolase inhibitor cyclohexyl carbamic acid 3'-carbamoyl-biphenyl-3-yl ester (URB597): effects on anandamide and oleylethanolamide deactivation. *J Pharmacol Exp Ther* 313: 352-358, 2005.
10. **Fu J, Gaetani S, Oveisi F, Lo Verme J, Serrano A, Rodriguez de Fonseca F, Rosengarth A, Luecke H, Di Giacomo B, Tarzia G, and Piomelli D.** Oleylethanolamide regulates feeding and body weight through activation of the nuclear receptor PPAR-alpha. *Nature* 425: 90-93, 2003.
11. **Gaetani S, Oveisi F, and Piomelli D.** Modulation of meal pattern in the rat by the anorexic lipid mediator oleylethanolamide. *Neuropsychopharmacology* 28: 1311-1316, 2003.
12. **Giuffrida A, Rodríguez de Fonseca F, and Piomelli D.** Quantification of bioactive acylethanolamides in rat plasma by electrospray mass spectrometry. *Anal Biochem* 280: 87-93, 2000.
13. **Hanus L, Gopher A, Almog S, and Mechoulam R.** Two new unsaturated fatty acid ethanolamides in brain that bind to the cannabinoid receptor. *J Med Chem* 36: 3032-3034, 1993.
14. **Hughes S, Zelus D, and Mouchiroud D.** Warm-blooded isochore structure in Nile crocodile and turtle. *Mol Biol Evol* 16: 1521-1527, 1999.
15. **Kersten S, Desvergne B, and Wahli W.** Roles of PPARs in health and disease. *Nature* 405: 421-424, 2000.
16. **Lo Verme J, Fu J, Astarita G, La Rana G, Russo R, Calignano A, and Piomelli D.** The nuclear receptor peroxisome proliferator-activated receptor-alpha

mediates the anti-inflammatory actions of palmitoylethanolamide. *Mol Pharmacol* 67: 15-19, 2005.

17. **Nielsen MJ, Petersen G, Astrup A, and Hansen HS.** Food intake is inhibited by oral oleoylethanolamide. *J Lipid Res* 45: 1027-1029, 2004.

18. **Osei-Hyiaman D, DePetrillo M, Pacher P, Liu J, Radaeva S, Batkai S, Harvey-White J, Mackie K, Offertaler L, Wang L, and Kunos G.** Endocannabinoid activation at hepatic CB1 receptors stimulates fatty acid synthesis and contributes to diet-induced obesity. *J Clin Invest* 115: 1298-1305, 2005.

19. **Oveisi F, Gaetani S, Eng KT, and Piomelli D.** Oleoylethanolamide inhibits food intake in free-feeding rats after oral administration. *Pharmacol Res* 49: 461-466, 2004.

20. **Piomelli D.** The molecular logic of endocannabinoid signalling. *Nat Rev Neurosci* 4: 873-884, 2003.

21. **Proulx K, Cota D, Castaneda TR, Tschop MH, D'Alessio DA, Tso P, Woods SC, and Seeley RJ.** Mechanisms of oleoylethanolamide-induced changes in feeding behavior and motor activity. *Am J Physiol Regul Integr Comp Physiol* 289: R729-737, 2005.

22. **Reggio PH.** Endocannabinoid structure-activity relationships for interaction at the cannabinoid receptors. *Prostaglandins Leukot Essent Fatty Acids* 66: 143-160., 2002.

23. **Ritter RC, Covasa M, and Matson CA.** Cholecystokinin: proofs and prospects for involvement in control of food intake and body weight. *Neuropeptides* 33: 387-399, 1999.

24. **Rodríguez de Fonseca F, Navarro M, Gómez R, Escuredo L, Nava F, Fu J, Murillo-Rodríguez E, Giuffrida A, LoVerme J, Gaetani S, Kathuria S, Gall C, and Piomelli D.** An anorexic lipid mediator regulated by feeding. *Nature* 414: 209-212, 2001.
25. **Secor SM and Diamond J.** Effects of meal size on postprandial responses in juvenile Burmese pythons (*Python molurus*). *Am J Physiol* 272: R902-912, 1997.
26. **Secor SM and Diamond J.** A vertebrate model of extreme physiological regulation. *Nature* 395: 659-662, 1998.
27. **Secor SM, Fehsenfeld D, Diamond J, and Adrian TE.** Responses of python gastrointestinal regulatory peptides to feeding. *Proc Natl Acad Sci U S A* 98: 13637-13642, 2001.
28. **Soderstrom K and Johnson F.** Zebra finch CB1 cannabinoid receptor: pharmacology and in vivo and in vitro effects of activation. *J Pharmacol Exp Ther* 297: 189-197, 2001.
29. **Soderstrom K, Leid M, Moore FL, and Murray TF.** Behavioral, pharmacological, and molecular characterization of an amphibian cannabinoid receptor. *J Neurochem* 75: 413-423, 2000.
30. **Ueda N, Okamoto Y, and Morishita J.** N-acylphosphatidylethanolamine-hydrolyzing phospholipase D: A novel enzyme of the beta-lactamase fold family releasing anandamide and other N-acylethanolamines. *Life Sci* 77: 1750-1758, 2005.
31. **Yamaguchi F, Macrae AD, and Brenner S.** Molecular cloning of two cannabinoid type 1-like receptor genes from the puffer fish *Fugu rubripes*. *Genomics* 35: 603-605, 1996.

## Figure Legends

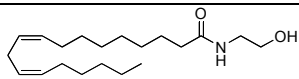
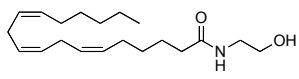
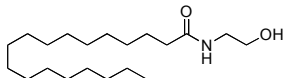
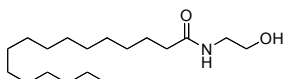
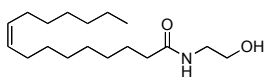
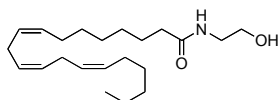
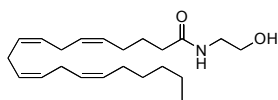
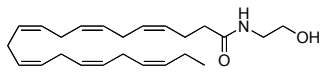
Scheme 1. Biosynthesis of OEA. Abbreviations: PE, phosphatidylethanolamine; PC, phosphatidylcholine; PA, phosphatidic acid; NAT, N-acyl transferase; NAPE-PLD, NAPE-specific phospholipase D.

Figure 1. Identification of OEA in python small intestine. A) LC chromatogram (top) and MS/MS spectrum (bottom) of native OEA from small intestine of fed pythons; B) LC chromatogram (top) and MS/MS spectrum (bottom) of synthetic OEA.

Figure 2. A) Representative LC/MS chromatograms illustrating (top) the elution of native OEA in the small intestine and (bottom) the elution of [<sup>2</sup>H<sub>4</sub>] OEA, added to the sample as internal standard. B) OEA levels in stomach, small intestine and colon of fasted (empty bars) and fed pythons (filled bars). Data represent the mean ± SEM of n=3-4 separate animals; \*\**P*<0.01 (two-way ANOVA followed by Bonferroni's post-hoc test); n.s., non significant.

Figure 3. A) Representative LC/MS chromatograms illustrating the identification of putative OEA precursors, NAPE1 (top) and NAPE2 (bottom) in the small intestine of fed pythons. B) Levels of NAPE1 (top) and NAPE 2 (bottom) in the gastrointestinal tract of fasting (empty bars) and fed (filled bars) pythons. Data represent the mean ± SEM of n=3-4 separate samples; \**P*<0.05 and \*\*\**P*<0.001 (two-way ANOVA followed by Bonferroni's post-hoc test); n.s., non significant.

Table1. Chemical structures and tissue levels (pmol/mg protein) of various FAEs in the gastrointestinal tract of *Python molurus*.

FAE	<i>m/z</i>	Structure	Feeding condition	Stomach	Small intestine	Colon
18:2, $\Delta^{9-12}$	346		Fasting	3±1	4±2	1±1
			Fed	2±2	325±101***	10±3
18:3, $\Delta^{6-9-12}$	344		Fasting	n.d.	n.d.	n.d.
			Fed	1±1	3±1	2±1
18:0	350		Fasting	11±1	5±2	8±5
			Fed	86±21	222±62**	42±14
16:0	322		Fasting	26±4	48±28	15±2
			Fed	115±24	335±137*	70±29
16:1, $\Delta^9$	320		Fasting	n.d.	n.d.	n.d.
			Fed	36±15	232±104*	3±3
20:3, $\Delta^{8-11-14}$	372		Fasting	9±1	4±1	18±14
			Fed	36±20	10±2	18±12
20:4, $\Delta^{5-8-11-14}$	370		Fasting	1±1	2±1	2±1
			Fed	12±9	17±6	7±5
22:6, $\Delta^{4-7-10-13-16-19}$	394		Fasting	n.d.	1±1	1±1
			Fed	8±5	14±6	n.d.

Values represent means ± SEM, n=3-4. \*\*\* $P$ <0.001, \*\* $P$ <0.01, \* $P$ <0.05; n.d. = non-detectable (two-way ANOVA followed by Bonferroni's post-hoc test, fed vs fasting).

Scheme 1.

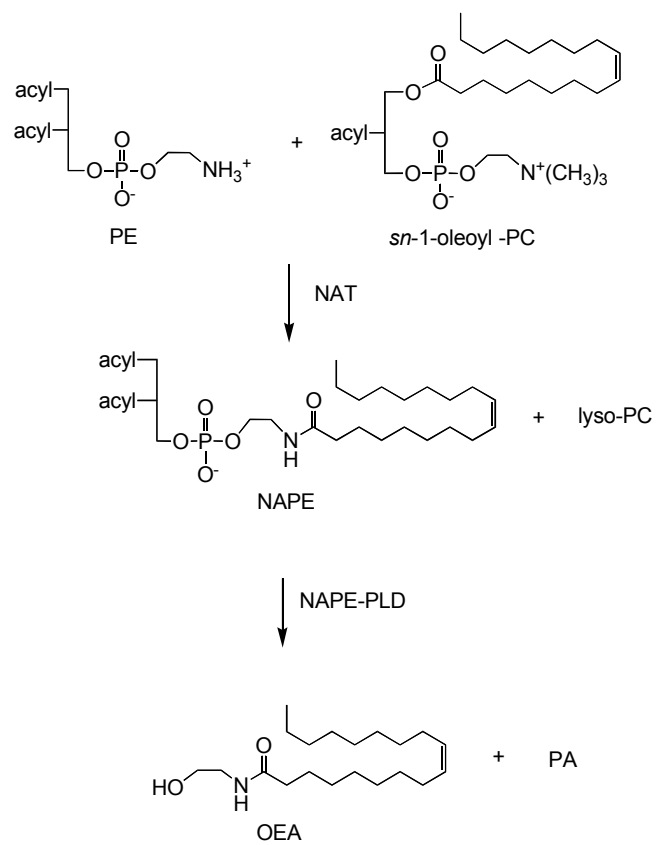


Figure 1.

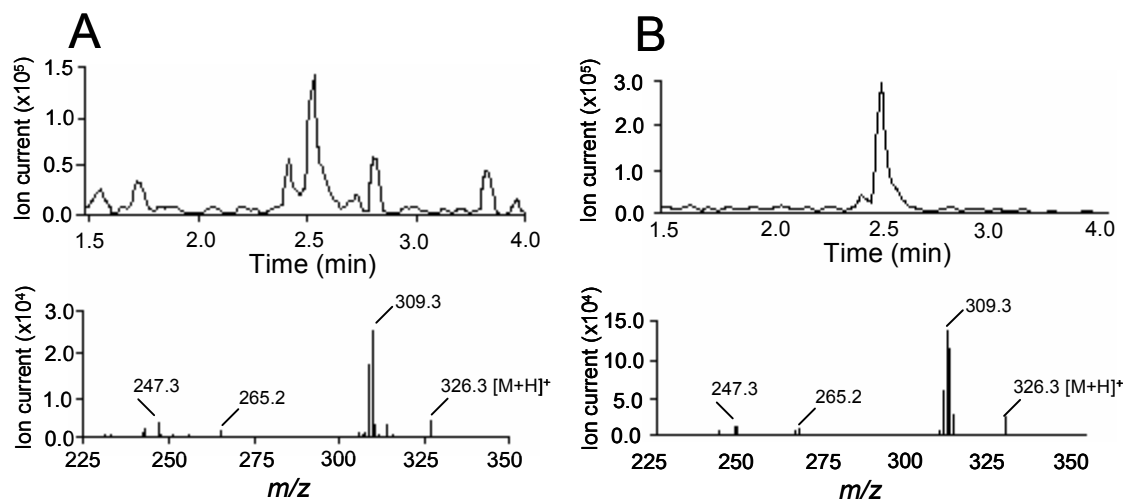


Figure 2.

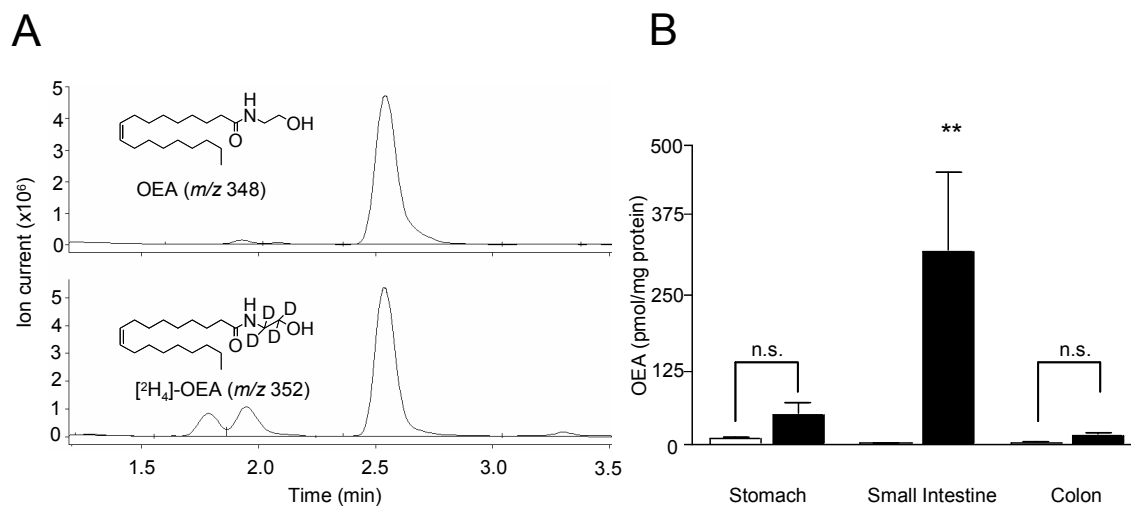


Figure 3.

